DarcyShale: An improved GRI method for more reliable measurements on low permeability samples

Roland Lenormand[1*], and *Sandra* Profice[2]

[1]CYDAREX, 31 avenue Gabriel Péri, 92500 Rueil-Malmaison, France
[2]TOTAL CSTJF, avenue Larribau, 64018 Pau Cedex, France

Abstract. In 1993 Luffel *et al.* proposed the Gas Research Institute (GRI) method for permeability measurement on crushed rock. In 2019, a benchmark analysis of GRI tests (SCA2019-016) revealed that the measured permeabilities were not reliable. The principal conclusion was that the thermal relaxation generated at the beginning of the test completely or partially hided the sample pressure response. In this paper we present an improved GRI method, named DarcyShale. By optimizing the device design, we minimized the experimental thermal effects at short times. We quantified the pressure variations not due to the viscous flow inside the rock with a highly permeable rock whose response should be instantaneous. We studied the impact of different gases and found that nitrogen is preferred to helium or krypton. We also show that mixing a fine powder with the crushed sample improves the quality of the measurement. As a quality control, we systematically checked that the signal amplitude agreed with the theoretical value computed from a porosity value obtained separately.

1 Introduction

In the early 90s, Luffel et al. [1] proposed an innovative method for measuring low permeabilities on crushed rocks or packs of drill cuttings, named Gas Research Institute (GRI) method. The test consists in imposing a gas pressure pulse on the particles and recording over time the response due to the gas flow in the pore network. The experimental signal is interpreted using either a numerical model or a simplified analytical solution. A GRI test being nothing more than a pycnometry test, the GRI device classically found in the industry is the pycnometry device sketched in Figure 1.

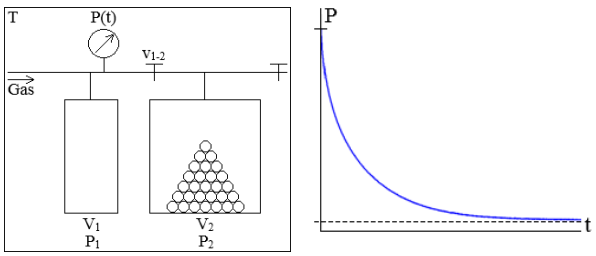

Figure 1 - GRI or pycnometry device and recorded pressure signal as function of time.

The sample is introduced in a chamber of volume V2 that is connected to a chamber of volume V1 via a valve v1-2. Initially, the valve v1-2 is closed and the pressure in the dead volume of the chamber V2 is at P2, as well as the pressure in the sample pore volume Vp. The test starts with the pressurization of the chamber V1 at a pressure P1 higher than the pressure P2, P2 being generally equal to the atmospheric pressure Patm. At time t=0, the valve v1-2 is opened, and the recording of the pressure transient P(t) is started simultaneously. The device is placed in a temperature-controlled oven or laboratory to keep its temperature T constant.

The option to work on rock particles is particularly appealing as it enables cost and time saving. Just a few grams of drill cuttings are enough for the test, which drastically reduces the test cost. Besides, the test duration is significantly shortened by both the increase of the medium exchange area with the invading gas and the decrease of the medium characteristic penetration depth [2]. Another argument proposed by Luffel *et al.* to promote the GRI method is the elimination of the coring-induced microfractures while crushing. The authors argue that such microfractures remain open even if the sample is confined and are thus responsible for a bias in the estimated matrix permeability.

As any method, the GRI method has limitations. The fact that a realistic confining pressure cannot be applied on the rock particles is as problematic as the existence of microfractures in a confined sample. Indeed, tight materials are highly sensitive to stress [3]. Moreover, Tinni et al. [4] refuted Luffel *et al.* argument that microfractures completely disappear when finely crushing. They detected microfractures in micro-computed tomography images of shale particles having sizes of 3.5 mm and 0.7 mm. From scanning electron microscopy images taken before and after crushing, Profice and Lenormand [5] even proved that crushing can generate microfractures. Crushing has the potential negative effect to damage the pore network [4]. Tinni *et al.* observed, for diverse rocks, that the permeability decreases as the mean particle diameter decreases. The mercury injection tests proved that this trend is not due to the gradual elimination of microfractures but to the modification of the pore throat size distribution.

* Corresponding author: roland.lenormand @cydarex.fr

Anisotropy is an additional factor affecting the estimated permeability. Contrary to tests on core plugs, tests on crushed samples do not give a directional permeability but a mean measurement, the gas penetrating the particles in the three space directions [3]. Simplifying the sample geometry by representing the polydisperse pack of particles by a monodisperse pack of spheres [2, 4, 5] or cylinders [1] possibly induces an error on the permeability [6]. However, as far as we know, quantifying this error has never been addressed rigorously in the current literature. Finally, the recorded pressure response is altered at short times by thermal effects created when opening the valve v1-2 [2, 5]. Sandra *et al.* [5] showed that these effects were one of the major causes explaining the significant dispersion of permeabilities determined for similar samples by different commercial laboratories equipped with GRI devices [7]. The pressure relaxation related to the gas flow and carrying information about the permeability is either partially or entirely hidden by the thermal relaxation.

The real nature of the thermal effects occurring at short times is not perfectly understood in the literature. They are usually qualified as Joule-Thomson effects [8]. A Joule-Thomson adiabatic gas expansion supposes a steady-state gas flow through a rigid and insulated tube obstructed by an obstacle, because of a pressure gradient along the tube [9]. In the case of a GRI test, the cross-section restriction introduced by the valve v1-2 acts as obstacle. However, the gas flow from the pressurized chamber V1 to the dead volume in the chamber V2 is never assimilated to a steady-state gas flow. It is generally assumed to be instantaneous [2, 4, 5]. A classic example of Joule-Thomson expansion is the injection of supercritical CO2 (high pressure and low temperature) in a depleted reservoir (low pressure and high temperature) [10]. The gas expansion engendered when opening the valve v1-2 resembles more a Joule-Gay Lussac adiabatic gas expansion. This type of expansion involves two rigid and insulated chambers isolated from each other by a valve, one chamber being pressurized and the other one being at a pressure equal to 0 [9]. The gas flow provoked by the valve opening is abrupt, as in a GRI test. The Joule-Thomson and Joule Gay-Lussac expansions are not identical in terms of Thermodynamics. Consequently, the gas temperature variations observed during these two expansions are not identical as well [9]. In a Joule-Gay Lussac expansion, the temperature decreases for most gases. Some exceptions exist. Helium, for instance, is subjected to temperature increase. In a Joule-Thomson expansion, the gas temperature increases or decreases depending on its initial value. The gas gets cooler only when its initial temperature is lower than a threshold temperature, named inversion temperature.

Some authors tried to model the heat exchanges between the gas and its environment during its expansion in a porous medium. Civan [6] started from the simulation work that App *et al.* [11] did to better understand the temperature variations observed at the field scale during oil and gas production tests. He developed an analytical model describing the gas flow under non-isothermal conditions by combining the equation of mass conservation, Darcy's law, the equation of energy conservation for the gas and the equation of energy conservation for the rock. This model considers the heat exchanges between the gas and the rock which originate from the fact that the gas has a temperature different from the rock temperature. It relates the changes in the gas temperature to energy loss by viscous dissipation and Joule-Thomson effects accompanying the gas expansion inside the rock. Suarez-Rivera et al. [12] went further in the modelling process by incorporating in their numerical model the various thermal phenomena taking place over the whole duration of a GRI test: heat exchanges between the gas and the matrix, heat exchanges between the gas and the device walls, heat transfer through the device walls. The authors identified the gas expansion right after valve opening to an adiabatic frictional gas flow through a tube having a constant cross-section. Such a flow is called Fanno flow.

The models applying in non-isothermal conditions are very complex and the true physics they are supposed to rely on is maybe still somewhat unclear. Our strategy regarding the thermal effects consisted in reducing the effects to keep the interpretation simple rather than modelling them.

In this paper we will first describe and discuss results obtained with a standard GRI apparatus that we have built. Then we will describe several improvements. The change of design allows a better determination of the average pressure during the relaxation leading to a more accurate determination. We have tested several gases: nitrogen; helium and krypton. We will discuss why the best results are obtained with nitrogen. We will also show that adding a powder to the crushed sample improves the accuracy of the measurements.

2 Results with the standard GRI method

We have built our own GRI device and analysed several experiments to discuss the limitations and the possible improvements.

2.1 Description of our GRI equipment

The volume V1 is 0.8 cc and volume V2 containing the sample is 8 cc. The maximum working pressure is 10 barg.

We used the pyrophyllite and shale samples described in the 2019 benchmark publication [5]. Porosities are respectively 0.045 and 0.13 frac. and liquid permeabilities around 20 and 10 nD. Crushed samples have a mean diameter of 1.7 mm. We have used both nitrogen and helium since these two gases were used in the benchmark.

For all the experiments described in this paper, permeabilities are determined by history matching of experimental data with the numerical model.

The model used in the interpretative procedure is based on two hypotheses. First, the crushed sample is assumed to be a monodisperse pack of homogeneous and isotropic

spheres. Second, the gas is supposed to follow the Boyle's law, to have a constant viscosity and to propagate in isothermal conditions. The model is a numerical model which considers the gas compressibility. Determining K_L and b values instead of a Kg value is not feasible since the two properties are correlated. As we will show at the end of this paper, the Klinkenberg correction is determined by performing several experiments at different pore pressures.

2.2 Results for L23

Figure 2 shows the recorded pressure for nitrogen and helium with the shale sample L23. The initial pressure in V1 is around 10 bar. After opening the valve, the pressure is around 1.5 bar, as it can be calculated using thermodynamics laws.

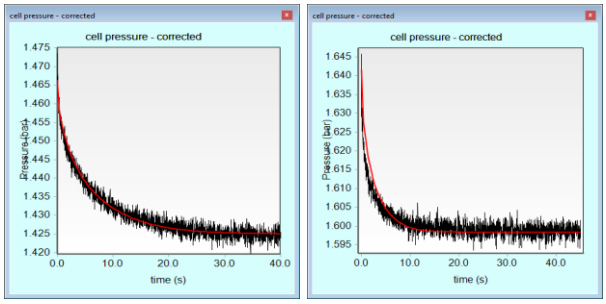

Figure 2 – L23: Recorded signal (black) during the relaxation and interpretation (red): a) with Nitrogen; b) with Helium

The interpreted permeabilities are 93 nD for nitrogen and 134 nD for helium. The difference is due to the Klinkenberg effect: the b coefficient being larger for helium than for nitrogen.

2.3 Results for Pyrophyllite

Figure 3 shows the results for the crushed pyrophyllite sample. The decreasing part of the curve is very short for N_2 (less than 0.5 s) and not visible for He. For N_2, Figure 4 shows the interpretation with Kg=500 nD, the gas permeability measured on plugs.

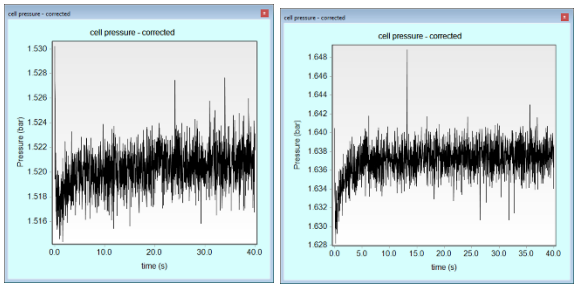

Figure 3 - Recorded signal during the relaxation with pyrophyllite sample: a) with Nitrogen; b) with Helium

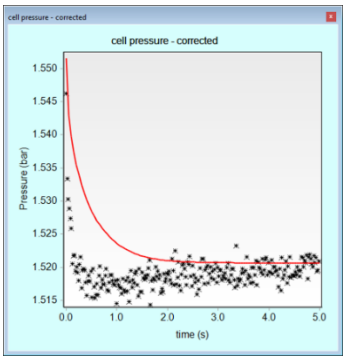

Figure 4 – pyrophyllite sample with N2: interpretation with Kg = 500 nD (in red)

2.4 Discussion of the results

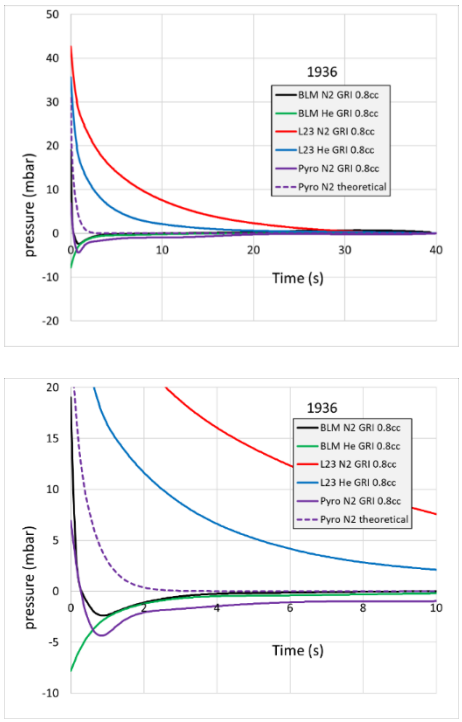

Figure 5 –– N_2 and He signals for L23 and pyrophyllite, normalized to the final pressure, and fitted with a spline function. Comparison to the signal recorded with the high permeability sample BLM.

Figure 5 show the signals for the shale L23 and pyrophyllite (N_2) compared to the signal obtained with a highly permeable brick sample (10 mD), called BLM. The signals are fitted with splines and shifted to finish at zero final pressure for all experiments.

With this standard equipment, we have two main problems:

2.4.1 Large variation of pressure in the sample

Figure 2 shows the pressure signal for experiment L23. The amplitude of the signal is around 50 mbar with an average pressure around 1.5 barg. But this measured pressure is the pressure outside the sample. For Klinkenberg correction, we need the average pore

pressure inside the sample. Initially the sample is at atmospheric pressure and the final pressure is 1.5 bar. The average relative pressure is 0.75 barg.

To determine accurately the Klinkenberg correction, we need average pore pressures in a large range of values, and around 10 barg seems a reasonable target. With 10 barg initial pressure, the final pressure is around 1.5 barg. Around 120 barg would be necessary to get a final pressure of 10 barg. Even in this case, the average pore pressure will be 5 barg (since the initial pressure is 0 barg).

The standard GRI method is not adapted for Klinkenberg correction and in the SCA benchmark [5], no company provided a Klinkenberg correction.

2.4.2 Abnormal relaxation at short times

For BLM with 10 mD permeability, the viscous relaxation inside the sample is too fast to be observed on the pressure record (less than 1 ms using numerical simulation). The recorded pressure transient is due to other mechanisms that we will discuss later.

This relaxation has two components: below 1s, decreasing for N_2 and increasing for He, possibly related to Joules-Thomson effect, since the effect is inverse for these two fluids, and after 1s, an increasing effect for both gases. We will assume that this "blank signal" related to the gas behaviour in the volumes and the intergranular space is always present and superimposed to the viscous relaxation in pores for other less permeable samples.

For the shale L23, due to the large porosity and low permeability, the signal due to the viscous flow is much larger than the blank signal, for both N_2 and He, and gas permeability can be accurately determined.

For the pyrophyllite sample with N_2, the dashed line represents the calculated response, assuming the gas permeability measured on the plugs (500 nD). The duration of this signal is comparable to the blank signal and the interpretation is not possible. We also can note that the shape of the signal shows a minimum, as for the blank. This shape of signal was also reported by services companies during the benchmark [5].

Now, we will show how we have solved these two problems by designing a new equipment that we call DarcyShale, by studying the effect of the nature of the gas and by adding a powder to fill the space between the grains of crushed porous material.

3 Improvements of the GRI method

3.1 Improvements of the design of the equipment

In the standard GRI design the volume V1 is small compared to volume V2 where the sample is placed

The advantage is a relaxation signal with a large amplitude since the volume outside the rock is small. The drawback is the limited pressure that can be reached.

The main modification of our equipment is to place the sample under pressure in the vessel V2 and then make a pulse decay by opening the valve on the vessel V1 at lower pressure (atmospheric pressure or vacuum). The pressure sensor measures the pressure in V2. The amplitude of the pulse can be adjusted by choosing the volume V1. With the same equipment as described previously (ratio V1/V2 = 1/10), when sample is initially at 10 barg, the final pressure is around 9 barg.

This configuration has several advantages:

1) A small total volume leading to a signal of large amplitude since V1 is small.

2) Pressure around 10 bar can be easily obtained, directly with a pressure regulator from a gas cylinder.

3) The average pressure is better defined (between 9 and 10 bar in the previous example instead of between 0 and 10 barg in the standard GRI equipment), leading to a better determination of the Klinkenberg coefficient.

Figure 6 shows the DarcyShale response of BLM (10 mD) with initial pressure at 10 bar in red to be compared to the black curve for the GRI at 1.5 barg final pressure. The sign of the blank response is inversed for the two equipment since V2 is under pressure in DarcyShale, but the amplitudes and durations are similar.

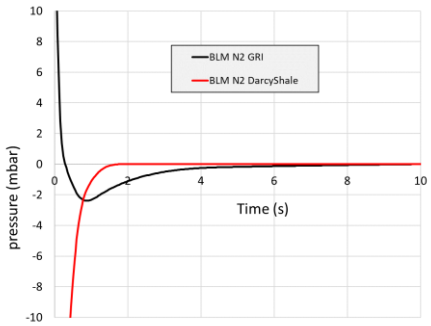

Figure 6 – Comparison of the blank BLM response for GRI and DarcyShale equipments.

To reduce the amplitude of the blank response, we have studied two parameters: the nature of gases and the effect of adding a fine powder between the grains of crushed material.

3.2 Effect of the nature of the gas

For the commercial measurements described in the 2019 SCA benchmark [5], both N_2 and He were used. Here we have studied these two gases. In addition, we also used krypton that has a larger molar mass and should lead to lower apparent permeabilities due to the Klinkenberg effect. For simplicity of interpretation, we have not tested CO2 that presents Kelvin condensation in small pores. However, this effect may present some interest and should be studied in the future.

The properties of the gases are given in Table 1 (from Air Liquid encyclopedia). We have added the properties of

xenon, but due to its cost, it has not been tested. By comparison with krypton, we do not think it presents an interest.

What is the effect of these gas properties on the experiments?

- Molar mass (and density) influences the inertial effects, the Reynolds number being proportional to the density. But we do not think that inertial effects are significant in our experiments.
- Molar mass also influences the apparent permeability through the coefficient b of the Klinkenberg effect. Using Klinkenberg law:

$$K_G = K_L\left(1 + \frac{b}{P_m}\right),$$

Where K_G is the apparent gas permeability, K_L the corrected (or liquid) permeability and Pm the average absolute pressure in the sample (generally, the arithmetic average between pressures at inlet and outlet of the sample). The expression of b is:

$$b = \frac{4c\mu}{r}\sqrt{\frac{\pi RT}{M}},$$

M is the gas molecular weight, μ the gas viscosity, c is a coefficient close to 1, r is the radius of the capillary tubes used to model the pore network (linked to permeability), T is absolute temperature and R is the universal gas law constant.

- The kinetic diameter is used to define the mean free path, also related to the Klinkenberg effect. This parameter is similar for the different gases.
- Viscosities are directly related to the transient flow, but the values are similar for all the gases.
- Joule-Thomson coefficient is related to the variation of temperature during a pressure drawdown through a porous medium of an orifice. The important point is that the effect is of opposite sign for N_2 and He.
- γ is the adiabatic expansion or compression coefficient. It differs for mono or diatomic gases.
- The specific heat is the amount of thermal energy accumulated per degree and unit of mass in the gas. Note that its value is higher for helium. However, the mass of helium in the vessels is much lower than for the other gases.
- Thermal conductivity characterized the rate of heat exchange through the gases, which is much higher for helium.

Table 1- Main physical properties of the gases at 25°C (from Air Liquid encyclopedia)

	unit	Helium	Nitrogen	Krypton	Xenon
Molar Mass		4	24	84	131
Viscosity	cP	0.0199	0.0178	0.0251	0.0212
compressibility factor		1.0005	0.9998	0.998	0.995
Density	Kg/m^3	0.168	1.15	3.43	5.4
Kinetic diameter	nm	0.260	0.364	0.360	
Thermal conductivity	mW/m.K	155.3	25.8	9.36	5.54
Specific heat	kJ/(kg.K)	5.19	1.04	0.25	0.16
Joule-Thomson coefficient	K/bar	- 0.07	0.23		
γ		1.69	1.4	1.67	1.68

We have tested the 3 gases: N_2, He and Kr on different samples without using additional powder between the grains of crushed porous material.

The non-porous glass beads are used, like BLM, as samples that should not present any relaxation. Figure 7 shows a small relaxation for helium, that increases for N_2 and Kr.

For the shale sample L4 (Figure 8), the amplitude of the signal is low for he, larger for N_2 and Kr. However, the difference with the glass beads is significant and the experiments can be interpreted, at least with N_2 and Kr.

For the pyrophyllite sample (Figure 9), the signal is very similar to the blank response of the glass beads and the experiments cannot be interpreted.

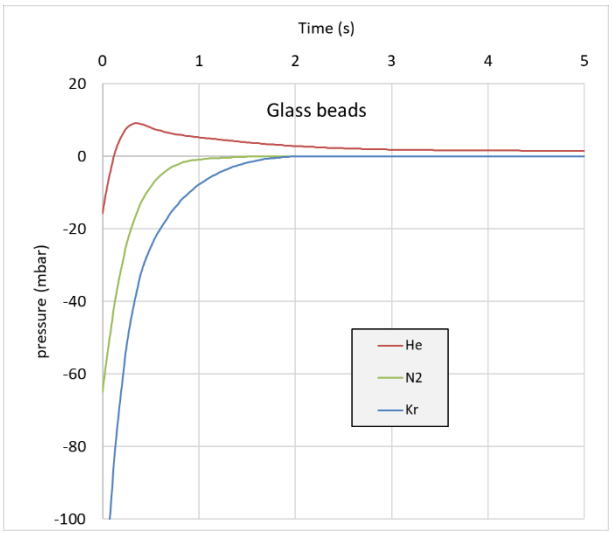

Figure 7 – 2 mm glass beads: Relaxations with the 3 gases.

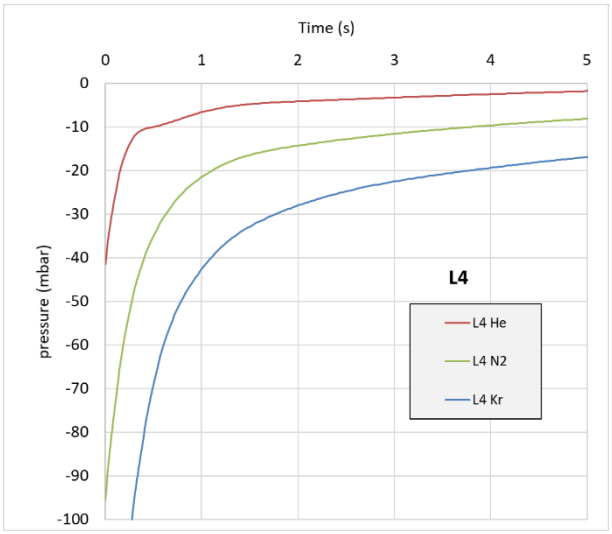

Figure 8 – Shale sample L4: Relaxations with the 3 gases

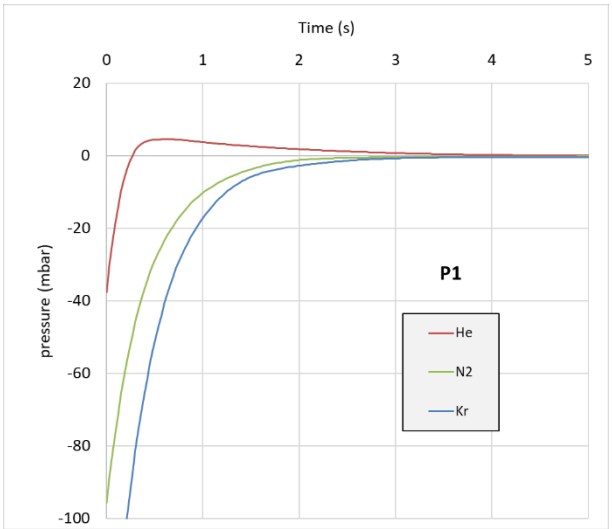

Figure 9 - Pyrophyllite: Relaxations with the 3 gases

As a conclusion, we see that He reduces the signals, both for the blank and for the samples. At the opposite, krypton leads to a large signal, both for the blank and for samples. Obviously, Helium must be discarded, at least for samples with permeabilities in the range of L4 or pyrophyllite. Krypton has no real advantage compared to N_2. We will see other results with adding powder in the next part of this paper that confirms that N_2 is the best gases for this type of measurement.

3.3 Adding powder to improve the pressure response

We will now discuss the effect of adding powder mixed with the grains of crushed rock.

Our first motivation was to reduce the dead volume around the crushed sample to improve the amplitude of the pressure signal. However, we quickly noticed that the effect of adding powder in reducing the blank response was more important than only a volume reduction.

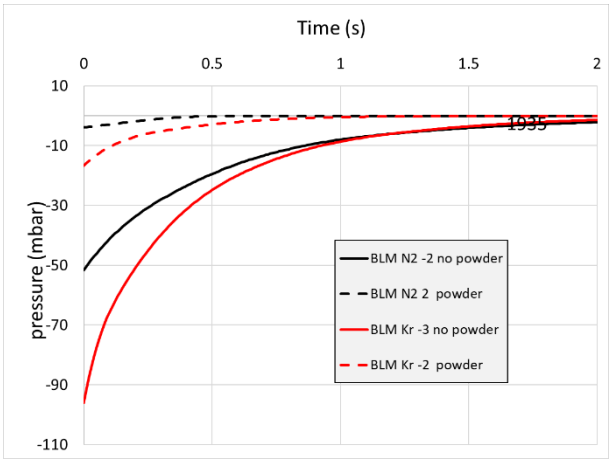

Figure 10 – Blank response of BLM with N_2 and Kr with and without powder.

Figure 10 shows the effect of a diatom earth powder (silica porous material) on the BLM with nitrogen and krypton. The powder has a large impact, reducing by a factor close to 10 the amplitude of the blank signal for both gases. Figure 11 shows a similar effect with 1 and 2 mm non-porous glass beads with krypton.

For all the experiments with powder, the amplitude of pressure at 1 second is reduced by a factor close to 10.

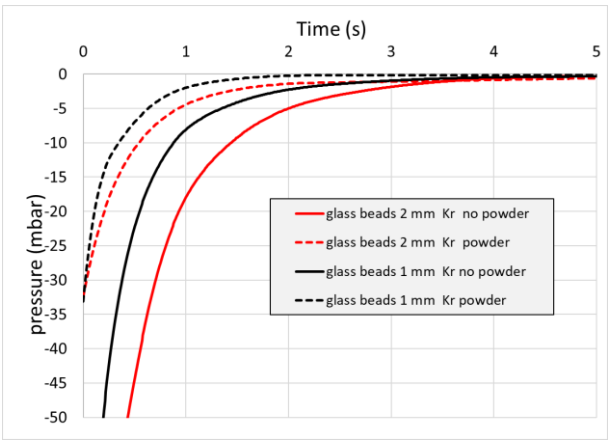

Figure 11 - Response for 1 and 2 mm glass beads with krypton with and without powder.

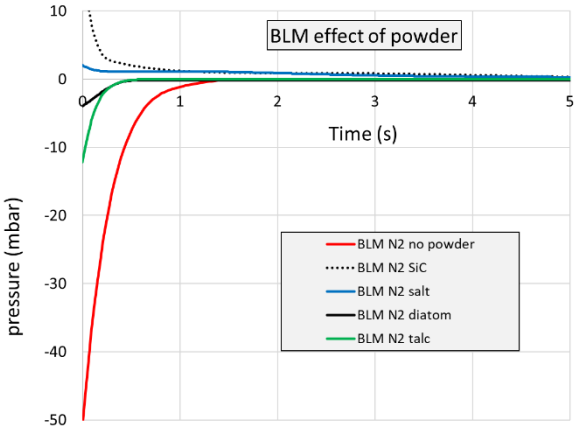

Figure 12 – Effect of the different powders on the presure response for the BLM sample with N_2.

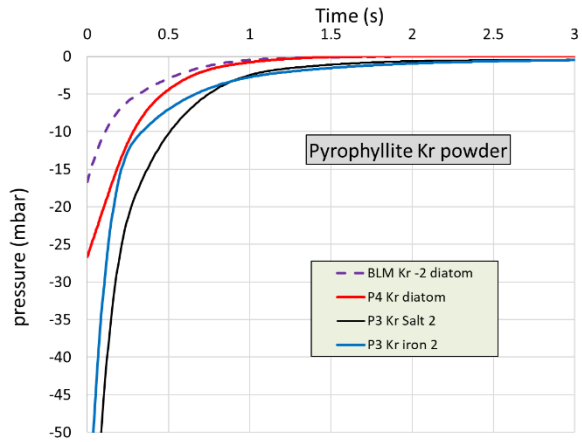

Figure 13 - Effect of the different powders on the presure response for pyrophyllite with krypton. The dashed black curve is the response of the BLM sample.

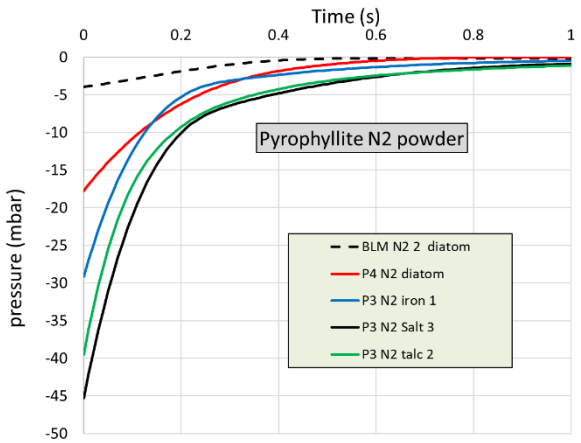

Figure 14 - Effect of the different powders on the presure response for pyrophyllite with nitrogen. The dashed black curve curve is the blank response of the BLM sample.

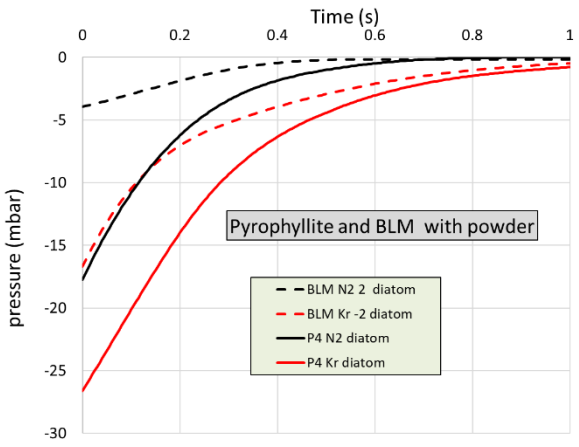

Figure 15 - Pyrophyllite (P4) and BLM with diatom powder: comparison of N_2 and Kr experiments.

The powder is well packed and fills all the empty space and we do not see any compaction after the experiment. In addition, we have tested the repeatability of the measurements.

We then studied the effect of the nature of the powder on the BLM sample with nitrogen (Figure 12) and pyrophyllite with krypton (Figure 13) and nitrogen (Figure 14).

Iron powder was tested expecting a larger effect for stabilizing the temperature due to its high thermal capacity. The purpose was to switch from an adiabatic toward an isothermal process. But there was no real difference with the other powder. The non-porous powders like SiC are more efficient than diatom earth but are difficult to use since any grain of SiC in a valve can damage the valve. The NaCl salt is efficient but difficult to operate since it does not "flow" easily between the grains of the crushed samples. Our first selection was talc that mixed very well with the sample particles. However, there are some questions about talc safety. We have opted for wheat flour that gives similar results.

Figure 15 shows the comparison between pyrophyllite (P4) and the blank BLM with nitrogen and krypton. As already discussed, the amplitude of the signal is larger and the relaxation time longer for krypton (red). However, the difference between the pyrophyllite signal and BLM is more pronounced for nitrogen (black). Therefore, we have selected nitrogen for the experiments.

4 Results with the improved DarcyShale equipment

With the DarcyShale equipment, we performed experiments with and without powder for pyrophyllite and the shale sample, and at different pressures to derive the Klinkenberg correction for the shale sample.

All the figures present the raw experimental pressure in black, and the numerical simulation in red.

4.1 Results with pyrophyllite (with nitrogen)

Figure 16 shows the result of an experiment without powder. The numerical simulation (in red) is performed using the real porosity of the sample (0.045 frac.). The numerical simulation cannot represent the experiment with the real value of porosity; a porosity 10 times larger is necessary to cover the amplitude of the signal. Without powder, the real signal is hidden by the thermal artifact over 1 second as previously described.

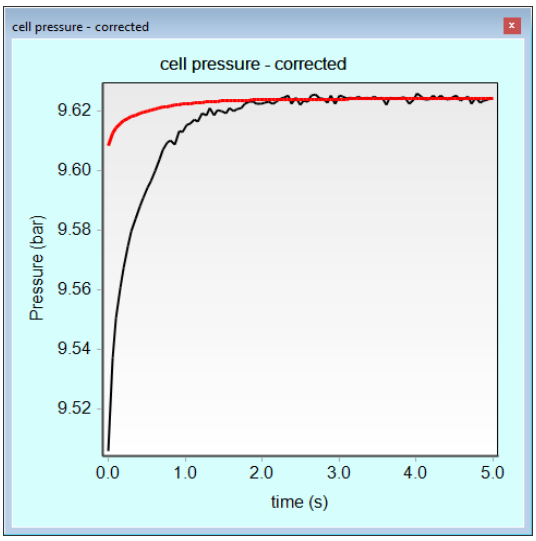

Figure 16 - Sample Pyrophyllite N2 without powder. Experimental data in black and numerical simulation in red with real porosity of the sample (0.045) and Kg = 100 nD.

With diatom powder (Figure 17), the signal seems noisier, but it is due to the scale of the axis. The numerical simulation can fit the experiment over the entire range of the relaxation using the real porosity.

This point is very important and can be consider as the main criterium for quality control of the experiment. With this criterium, the experiment without powder cannot be qualified.

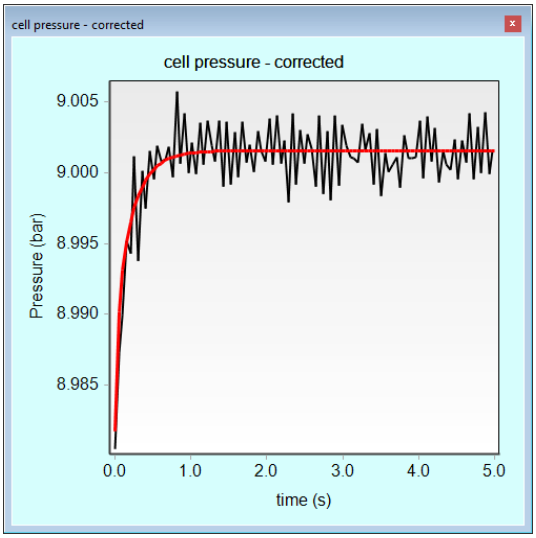

Figure 17 - Sample Pyrophyllite N2 with diatom powder. Experimental data in black and numerical simulation in red with real porosity of the sample (0.045) and Kg = 250 nD.

4.2 Results with the shale sample L (with krypton)

The signal is better for shale L since its permeability is lower (longer relaxation time) and porosity higher (higher amplitude of the signal). However, the comparison with and without powder is similar to the pyrophyllite.

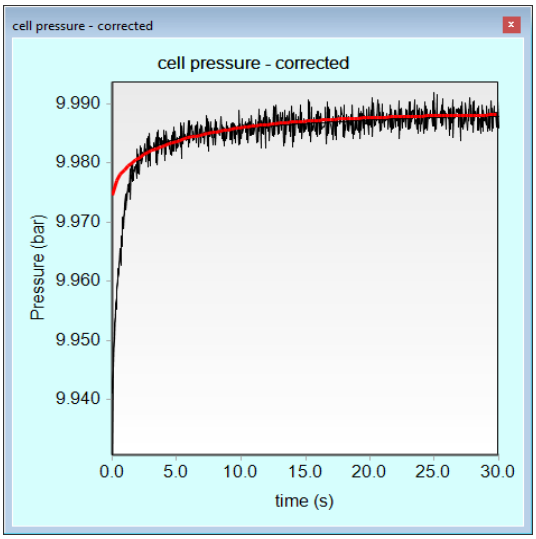

Figure 18 – Sample L4 without powder. Experimental data in black and numerical simulation in red with real porosity of the sample (0.13) and Kg = 25 nD.

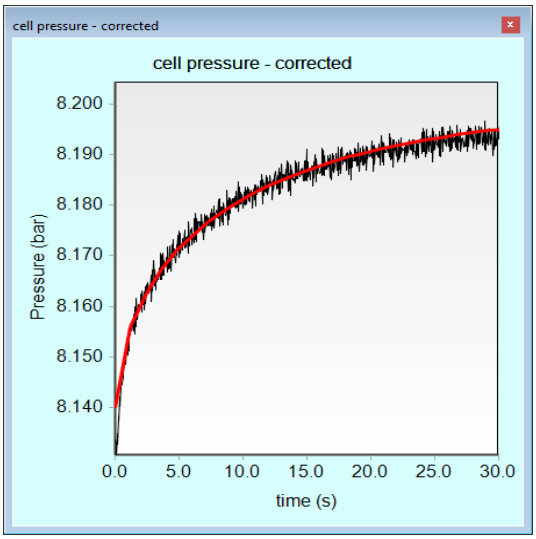

Figure 19 - Sample L4 with diatom powder. Experimental data in black and numerical simulation in red with real porosity of the sample (0.13) and Kg = 17 nD.

Without powder (Figure 18), the simulation cannot represent the experiment: the amplitude is too small when using the real porosity of the sample and the result is not acceptable for quality control.

With powder (Figure 19), the agreement is very good between the experiment and the simulation over the entire range of the relaxation using the real porosity of the sample.

Klinkenberg plot for shale sample

Figure 20 shows the results for the shale sample with diatom earth at different pressures to derive the Klinkenberg correction. The results with the three gases used in the study are plotted. The measurements have been checked for quality control as described previously. The pressure P is the average between initial and final pressures in the sample. The lower values in 1/P correspond to initial pressure around 10 barg and the highest value to initial pressure around 1.3 barg. Below this pressure, the signal is too noisy to be interpreted.

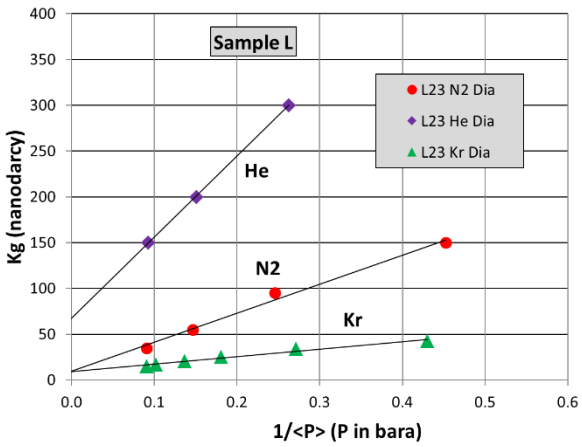

Figure 20 - Klinkenberg plot for L crushed samples with different gases.

For all the gases, the gas permeabilities follow a linear law as function of 1/Pm as expected from Klinkenberg theory. For this L sample, with low permeability and high porosity, the results with helium are acceptable. Extrapolated values for 1/Pm=0 agree for nitrogen and krypton but differ for helium. As already discussed, helium leads to very short relaxation times and is not recommended.

For N_2 and Kr, the extrapolated absolute permeabilities are respectively 9.6 and 9.4 nD and the b coefficients 33 and 8.6 bar. If we take as reference the b value for nitrogen, the theory predicts b=25 bar for krypton, higher than the experimental value. We have no explanation for this difference. It cannot be related to a bad flushing of the sample after nitrogen or helium experiment since the b would have been higher. It has been reported that the Klinkenberg correction formulated at the scale of the sample was not valid for transient flow [8]. Further study would need to re-interpret all the experiments with Klinkenberg effects calculated at the grid scale in the numerical simulations. So far, we consider that this difference is within the range of the accuracy of the method.

5 Discussion

We will present a tentative explanation of the role of the powder to reduce the "blank" relaxation at the beginning of the experiment. A proven theory would need additional measurements, high speed record of temperature in the vessels, measurement of powder packing permeability and modelling using non-isothermal flow with thermodynamics effects. This is not in our capacities and not the purpose of this study.

Let us consider Figure 1 with the crushed sample at pressure P2=10 barg in volume V2 and the volume V1 at atmospheric pressure. Gas is nitrogen. After opening the valve, we assume that the volumes are such that the pressures equilibrate at 9 barg.

Now, we must consider the thermal effects. We can consider two extreme cases:

1) **Pressure equilibrium**: A very fast change of pressure when opening the valve; no pressure drop in the valve and in the space between the grains of crushed sample (no powder). We assume that there is no thermal exchange between the gas and the container at the opening of the valve. Therefore, the experiment is an adiabatic expansion in V2 (10 to 9 barg) and compression in V1 (0 to 9 barg). The actual physics is more complicated since there is a transfer of gas between the two vessels. Neglecting the transfer of gas, the theoretical calculation leads to a decrease of temperature of 8°C in V2 corresponding to a decrease of pressure of 270 mbar, and an increase of temperature of 280°C in V1. The corresponding increase of pressure for V1 is 9.3 bar. In this process, the equilibrium of pressure is much faster that the temperature equilibrium. The pressure quickly equilibrates but the temperature needs more time and is function of the heat
2) accumulated (mass of gas and heat capacity) and the rate of heat transfer (heat conductivity).

2) **Thermal equilibrium**: if we consider now a very slow process, for instance by connecting the two vessels through a needle valve, the pressures will not be in equilibrium between the two vessels, but the temperatures will equilibrate by thermal conductivity in the gas. However, with such a slow process, it would be impossible to study the transient inside the rock.

Without powder, the process corresponds to the first case of fast pressure equilibrium in the two volumes. During an experiment, we record the pressure in V2, and we observe the decrease of pressure reaching 100 mbar after around 0.1 second., in agreement with the theoretical calculation of 270 mbar at time t=0.

Adding powder involves the second case of thermal equilibrium. The powder slows down the pressure exchange and allows the temperature to equilibrate over a few tens of second, fast enough to allow the observation of the transient of pressure by viscous flow in the sample.

The thermal equilibrium is much faster with helium, which presents a low thermal capacity (due to its low mass, even if its thermal capacity is high) and a high thermal conductivity. However, helium has the drawback to decrease the apparent permeability, and therefore reduces the relaxation of the sample due to the Klinkenberg effect. On the other hand, krypton has a much higher thermal capacity and lower thermal conductivity than helium. Thermal equilibrium is much slower. Even if the apparent permeability is lower with krypton, the thermal effect impacts the quality of the measurement.

As already shown, nitrogen, with properties between helium and krypton, gives the best results.

6 Conclusions

We first discussed the limitations of the standard GRI method using an apparatus that we have built:

- Large difference between initial and final pressures in the sample not allowing the Klinkenberg correction.
- Thermal effects at the beginning of experiments that hides the short transient effects due to the viscous flow in the sample.

This paper presents an improved GRI method, named DarcyShale:

- We minimized the experimental artifacts at short times by optimizing the device design, minimizing the dead volumes and the procedure for realizing the pulse decay.

- We studied the impact of the gas nature and highlighted that nitrogen is preferred to helium or krypton.
- We have also shown that mixing a fine powder with the crushed sample improves the quality of the measurement. A tentative explanation was given.
- We quantified the pressure variations due to the residual artifacts with a highly permeable rock whose response should be instantaneous.
- As a quality control, we systematically checked that the signal amplitude agreed with the theoretical value computed from a porosity value obtained separately.

7 Nomenclature

b	bar	Klinkenberg coefficient
c	-	Coefficient close to 1 in b Klinkenberg coefficient
K_G	mD	Gas Permeability
K_L	mD	Klinkenberg corrected permeability
M	$g.mol^{-1}$	Molecular weight
P	bar	Pressure
r	m	Radius in the b formula
R	$J.mol^{-1}.K^{-1}$	Universal gas law constant
t	s	Time
V	cm^3	Volume
μ	cP	Viscosity

8 References

1. D. L. Luffel, C. W. Hopkins and P. D. Shettler, “Matrix permeability measurement of gas productive shales”, presented at the SPE Annu. Tech. Conf. and Exhib., Houston, TX, USA, Oct. 3 - 6, 1993, Paper SPE 26633.
2. S. Profice, D. Lasseux, Y. Jannot, N. Jebara and G. Hamon, “Permeability, porosity and Klinkenberg coefficient determination on crushed porous media”, presented at the SCA Int. Symp., Austin, TX, USA, Sep. 18 - 21, 2011, Paper SCA2011-32.
3. O. Kwon, A. K. Kronenberg, A. F. Gangi and B. Johnson, “Permeability of Wilcox shale and its effective pressure law”, *J. Geophys. Res.-Atmos.*, vol. 106, n° B9, pp. 19,339 - 19,353, Sep. 10, 2001, doi: 10.1029/2001JB000273.
4. A. Tinni, E. Fathi, R. Agarwal, C. Sondergeld, Y. Akkutlu and C. Rai, “Shale permeability measurements on plugs and crushed samples”, presented at the SPE Can. Unconventional Resources Conf., Calgary, AB, Canada, Oct. 30 - Nov. 1, 2012, Paper SPE 162235.
5. S. Profice and R. Lenormand, “Low permeability measurement on crushed rock: insights”, presented at the SCA Int. Symp., Pau, France, Sep. 26 - 30, 2019, Paper SCA2019-016.
6. F. Civan, “Can gas permeability of fractured shale be determined accurately by testing core plugs, drill cuttings and crushed samples?”, presented at the SPE/AAPG/SEG Unconventional Resources Technol. Conf., Austin, TX, USA, Jul. 24 - 26, 2017, Paper URTeC: 2666389.
7. Q. R. Passey, K. M. Bohacs, W. L. Esch, R. Klimentidis and S. Sinah, “From oil-prone source rock to gas-producing shale reservoir - Geologic and petrophysical characterization of unconventional shale-gas reservoirs”, presented at the CPS/SPE Int. Oil & Gas Conf. and Exhib., Beijing, China, Jun. 8 - 10, 2010, Paper SPE 131350.
8. R. Lenormand, F. Bauget and G. Ringot, “Permeability measurement on small rock samples”, presented at the SCA Int. Symp., Halifax, NS, Canada, Oct. 4 - 7, 2010, Paper SCA2010-A073.
9. J.-P. Qadri. (2008-2009). T4 - Appendice 1 - Détentes de Joule - Bilans énergétique et entropique [Online]. Available : http://pcsi-unautreregard.over-blog.com/
10. D. R. Maloney and M. Briceno, “Experimental investigation of cooling effects resulting from injecting high pressure liquid or supercritical CO_2 into a low pressure gas reservoir”, presented at the SCA Int. Symp., Abu Dhabi, UAE, Oct. 29 - Nov. 2, 2008, Paper SCA2008-40.
11. J. F. App, “Field cases: nonisothermal behavior due to Joule-Thomson and transient fluid expansion/compression effects”, presented at the SPE Annu. Tech. Conf. and Exhib., New Orleans, LA, USA, Oct. 4 - 7, 2009, Paper SPE 124338.
12. R. Suarez-Rivera, M. Chertov, D. Willberg, S. Green and J. Keller, “Understanding permeability measurements in tight shales promotes enhanced determination of reservoir quality”, presented at the SPE Can. Unconventional Resources Conf., Calgary, AB, Canada, Oct. 30 - Nov. 1, 2012, Paper SPE 162816.